*Supplementary Material*

# Antifungal activity of Co(II) and Cu(II) complexes containing 1,3-bis(benzotriazol-1-yl)-propan-2-ol on the growth and virulence traits of fluconazole-resistant *Candida* species: Synthesis, DFT calculations, and biological activity

Ricardo A. Murcia-Galan[1], Sandra M. Durán[2], Sandra M. Leal-Pinto[2], Martha V. Roa-Cordero[2], Jose D. Vargas[2], Laura V. Herrera[3], Alvaro Muñoz-Castro[4], Desmond MacLeod-Carey[5], Tonny W. Naranjo[6,7], Peter L. Rodríguez-Kessler,[8] John J. Hurtado[1*]

[1]Grupo de investigación en Química Inorgánica, Catálisis y Bioinorgánica, Departamento de Química, Universidad de los Andes, Carrera 1 No. 18A-12, 111711, Bogotá-Colombia; ra.murcia@uniandes.edu.co; jj.hurtado@uniandes.edu.co
[2]Universidad de Santander, Facultad de Ciencias Médicas y de la Salud, Calle 70 No. 55-210, Bucaramanga-Colombia; sandramduranbarajas@gmail.com sa.leal@mail.udes.edu.co; ma.roa@mail.udes.edu.co; vargasjosedavid.7.3@gmail.com
[3]Grupo Sistema Estomatognático y Morfofisiología (SEMF). Departamento de Ciencias Básicas, Universidad Santo Tomás seccional Bucaramanga, cra 27 No. 180-395, Bucaramanga-Colombia; laura.herrera01@ustabuca.edu.co
[4]Facultad de Ingeniería, Arquitectura y Diseño, Universidad San Sebastián, Bellavista 7, Santiago, 8420524 Chile; alvaro.munozc@uss.cl
[5]Universidad Autónoma de Chile, Facultad de Ingeniería, Instituto de Ciencias Químicas Aplicadas, Inorganic Chemistry and Molecular Materials Center, El Llano Subercaseaux 2801, Santiago, Chile; desmond.macleod@uautonoma.cl
[6] Corporación para Investigaciones Biológicas (CIB), Experimental and Medical Micology Group, Medellin 050010, Colombia; tnaranjo@cib.org.co
[7] Universidad Pontificia Bolivariana, Facultad de Medicina, Medellín 050034,Colombia; tnaranjo@cib.org.co
[8]Centro de Investigaciones en Óptica A.C., Loma del Bosque 115, Col. Lomas del Campestre, León, Guanajuato, 37150, México; plkessler@cio.mx
* Correspondence: jj.hurtado@uniandes.edu.co; Tel.: +57-1-3394949 (ext. 3468), ORCID: https://orcid.org/0000-0002-0511-9719

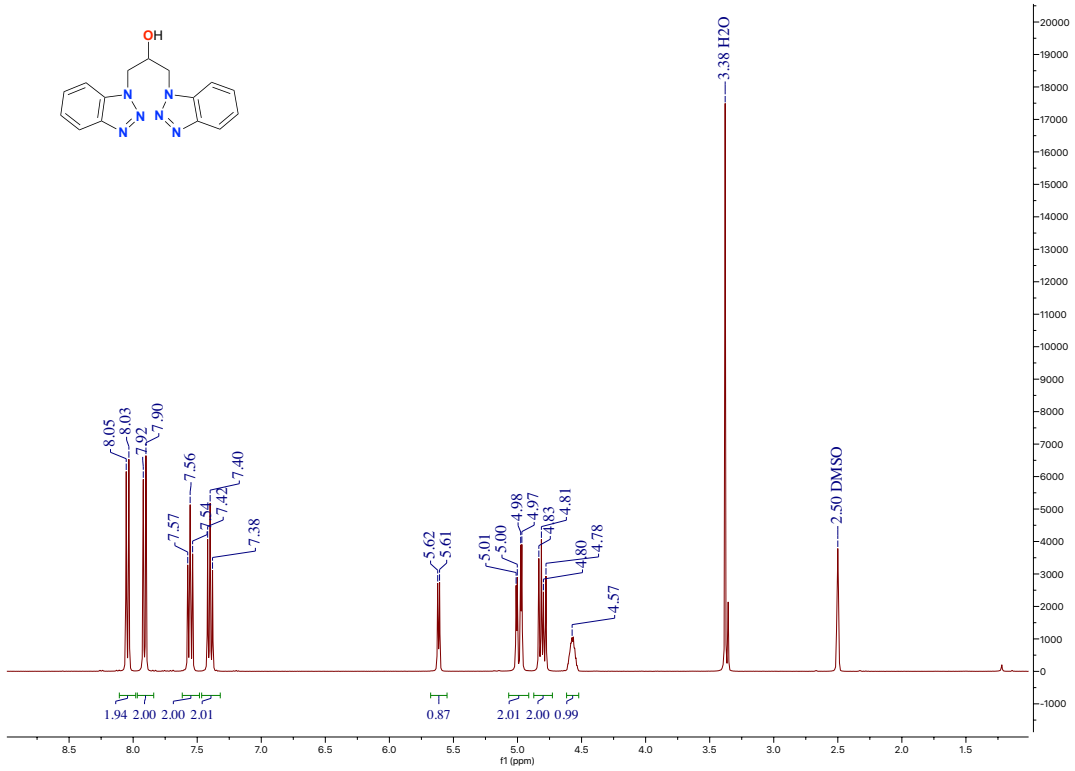


**Figure S1.** $^{1}$H NMR spectrum of 1,3-bis(benzotriazole-1-yl)propan-2-ol (**1**) in DMSO-$d_6$

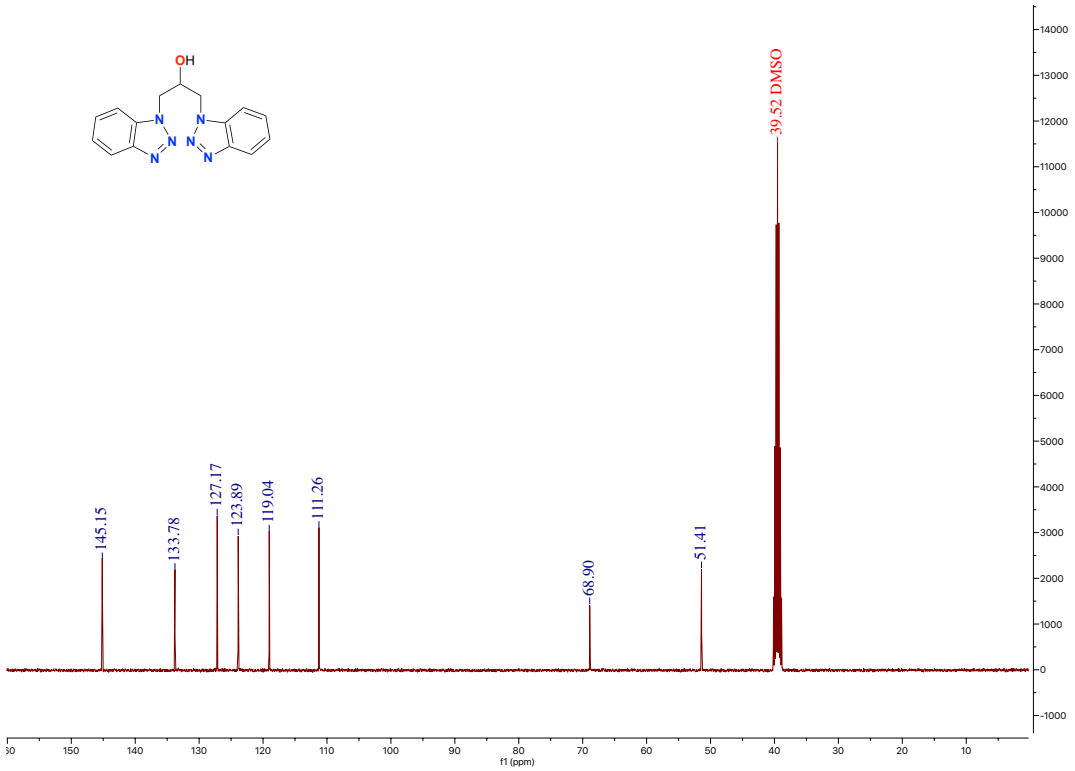


**Figure S2.** $^{13}$C NMR spectrum of 1,3-bis(benzotriazole-1-yl)propan-2-ol (**1**) in DMSO-$d_6$

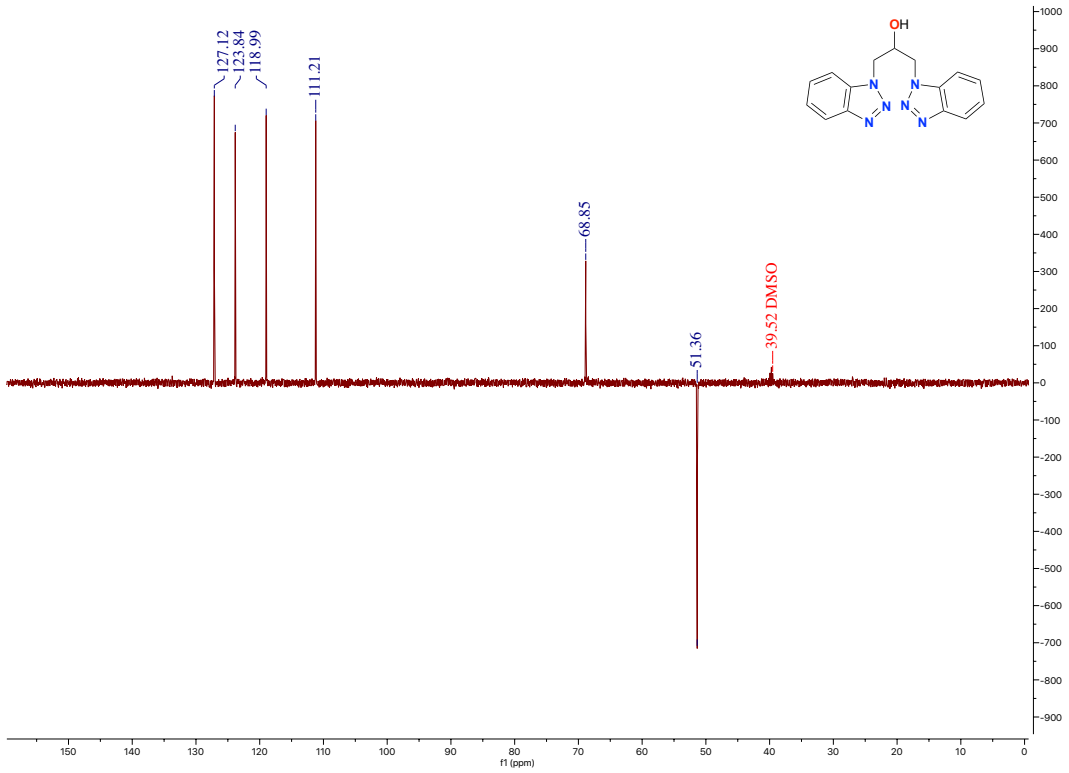


**Figure S3.** DEPT NMR spectrum of 1,3-bis(benzotriazole-1-yl)propan-2-ol (**1**) in DMSO-$d_6$

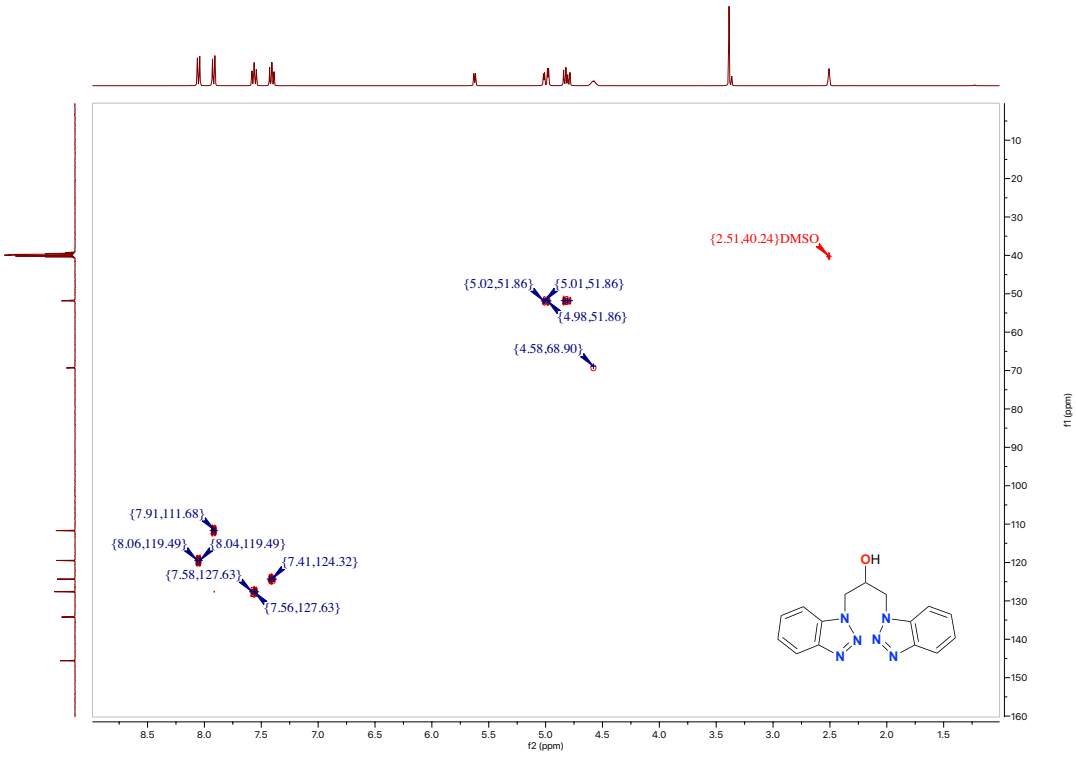


**Figure S4.** HSQC NMR spectrum of 1,3-bis(benzotriazole-1-yl)propan-2-ol (**1**) in DMSO-$d_6$

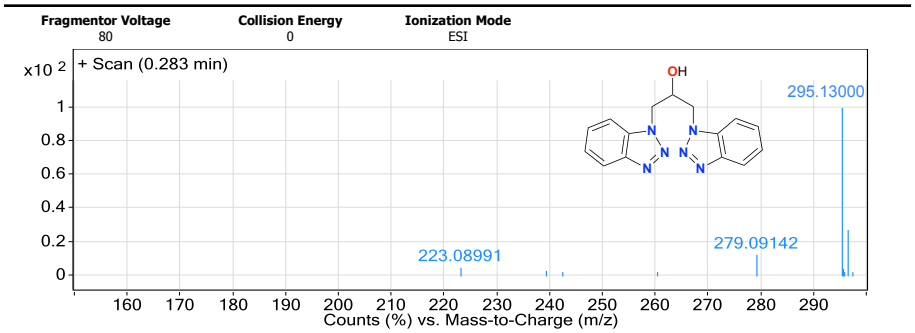


**Figure S5.** MS spectrum of 1,3-bis(benzotriazole-1-yl)propan-2-ol (**1**)

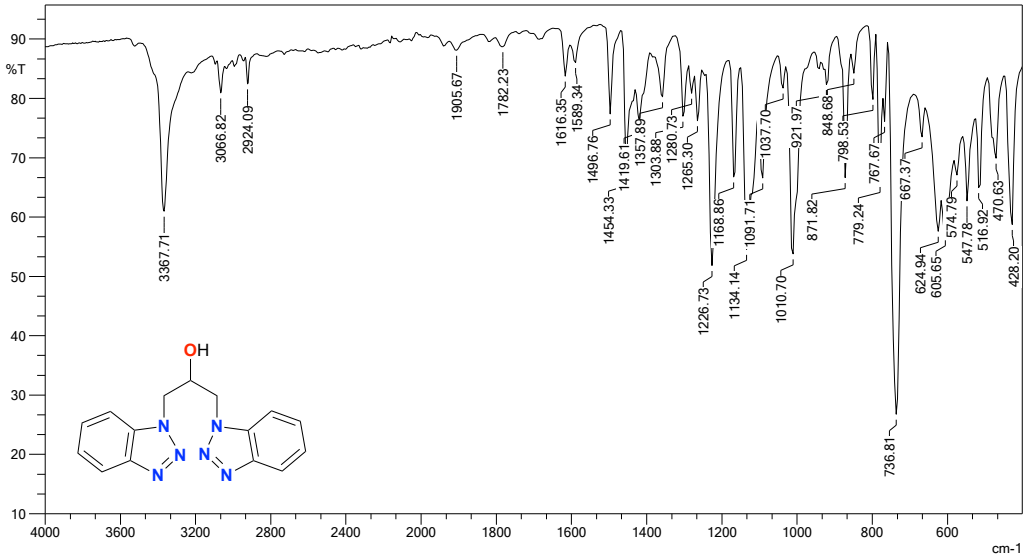


**Figure S6**. FT-IR (ATR) spectrum of 1,3-bis(benzotriazole-1-yl)propan-2-ol (**1**)

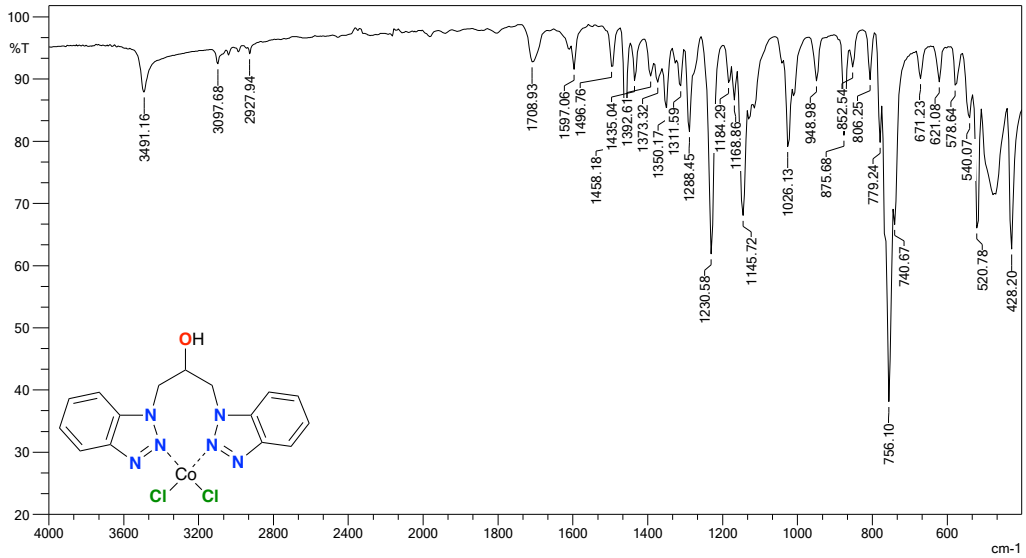


**Figure S7**. FT-IR (ATR) spectrum of dichloro[1,3-bis(benzotriazole-1-yl)propan-2-ol-N,N']cobalt(II) (**2**)

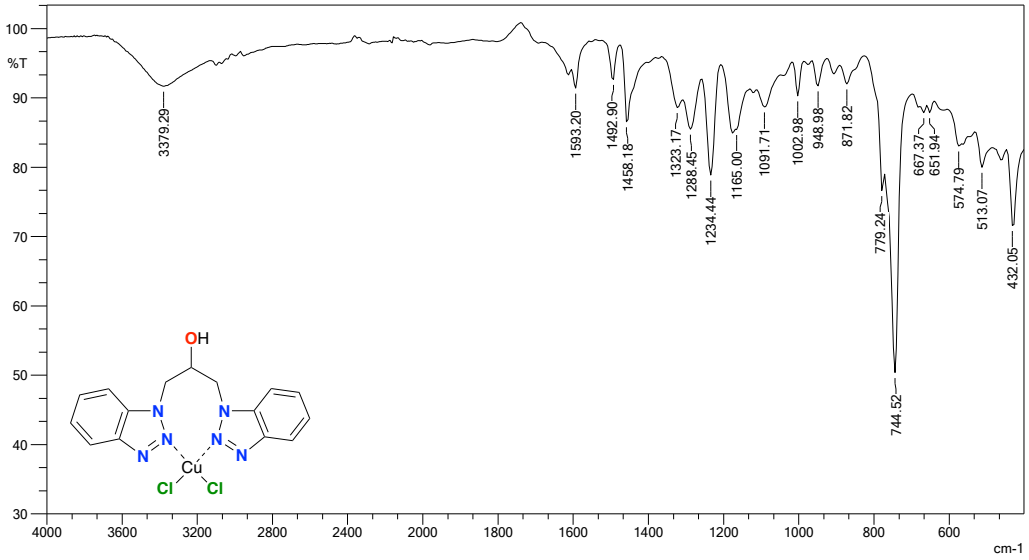


**Figure S8**. FT-IR (ATR) spectrum of dichloro[1,3-bis(benzotriazole-1-yl)propan-2-ol-N,N']copper(II) (**3**)

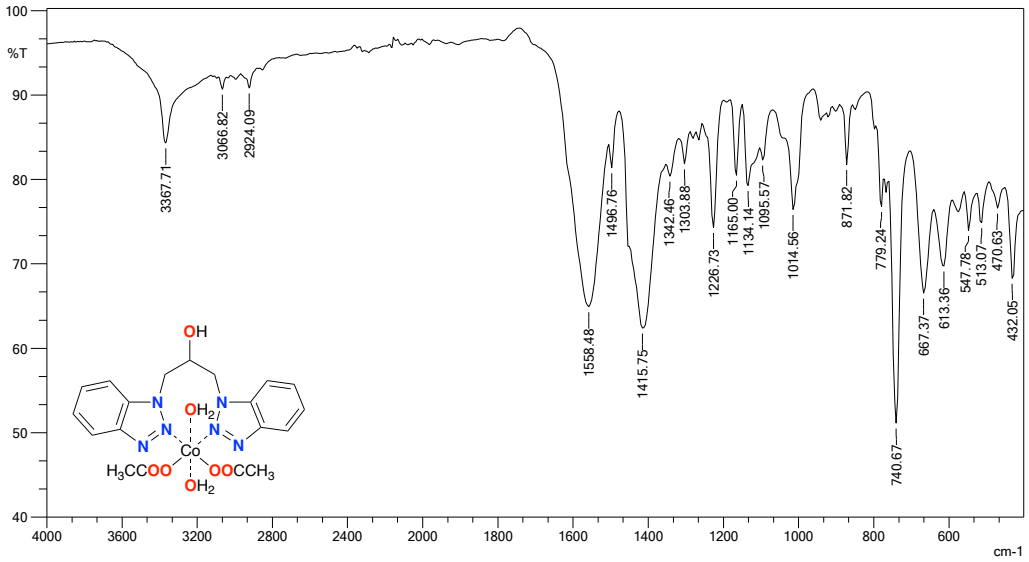


**Figure S9**. FT-IR (ATR) spectrum of diacetate-diaqua-[1,3-bis(benzotriazole-1-yl)propan-2-ol-N,N']cobalt(II) (**4**)

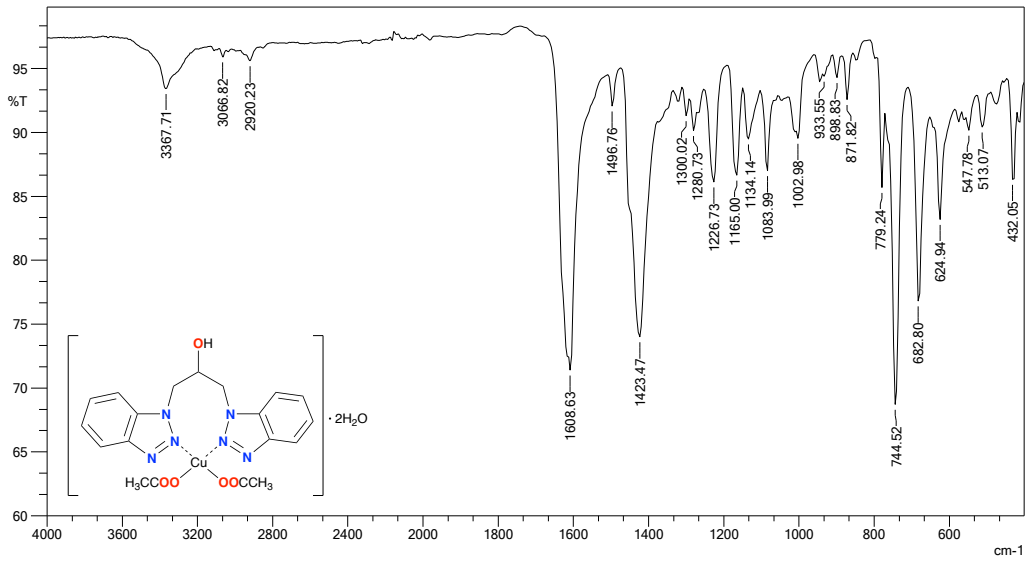


**Figure S10**. FT-IR (ATR) spectrum of diacetate[1,3-bis(benzotriazole-1-yl)propan-2-ol-N,N']copper(II) dihydrated (**5**)

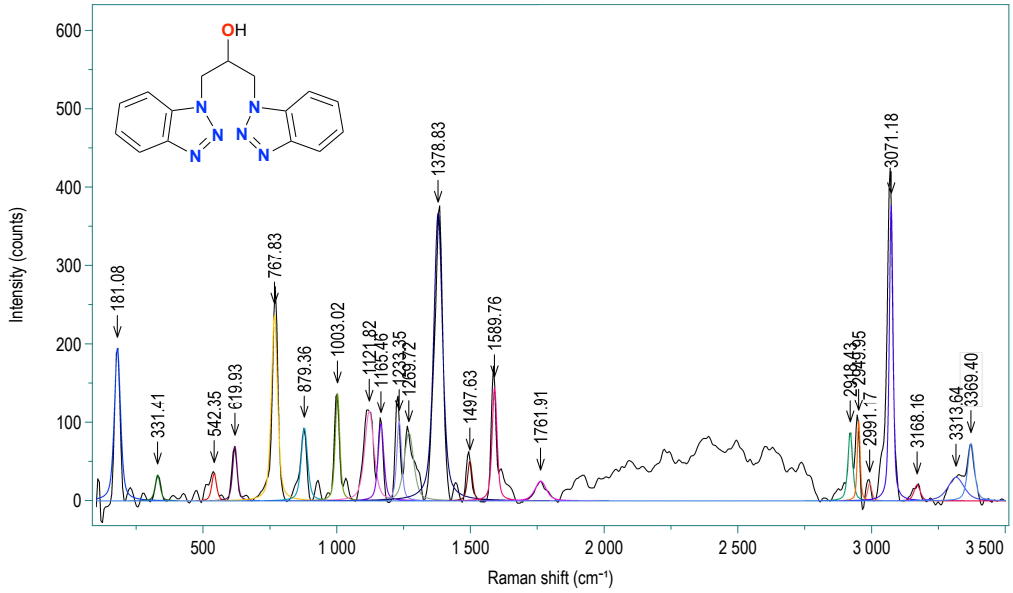


**Figure S11**. Raman spectrum of 1,3-bis(benzotriazole-1-yl)propan-2-ol (**1**)

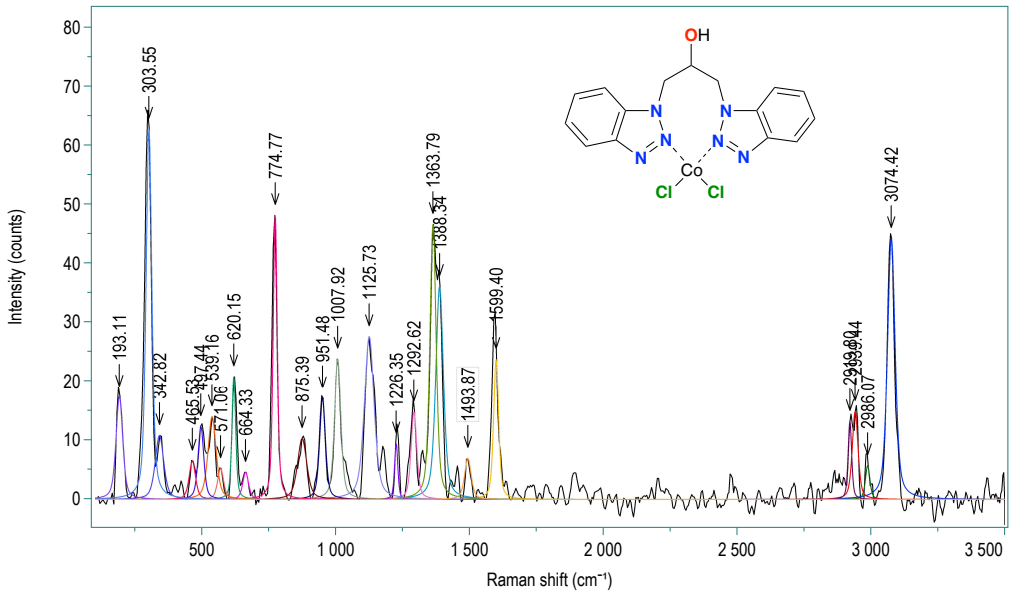


**Figure S12**. Raman spectrum of dichloro[1,3-bis(benzotriazole-1-yl)propan-2-ol-N,N']cobalt(II) (**2**)

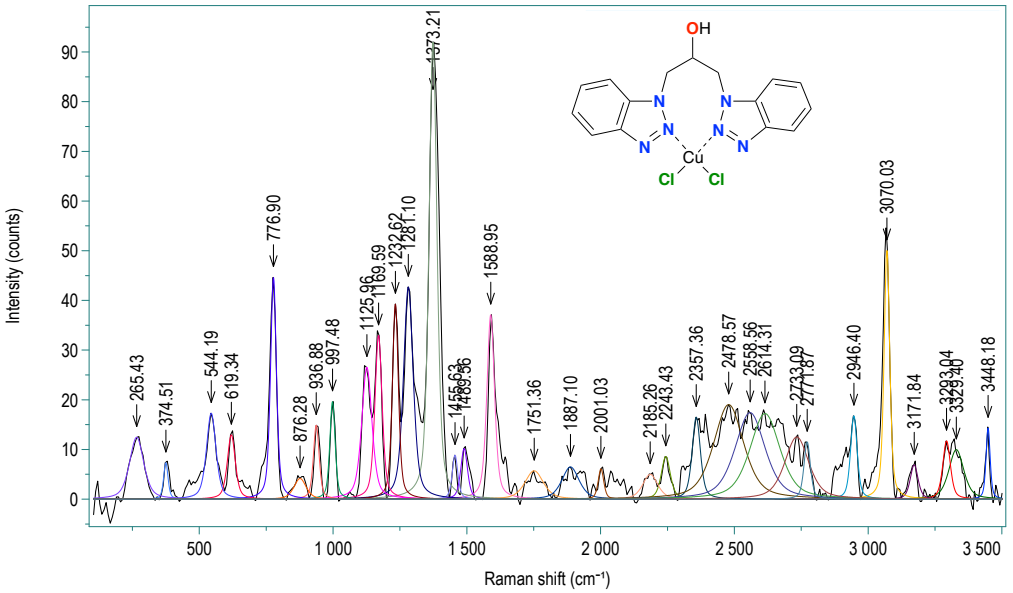


**Figure S13**. Raman spectrum of dichloro[1,3-bis(benzotriazole-1-yl)propan-2-ol-N,N']copper(II) (**3**)

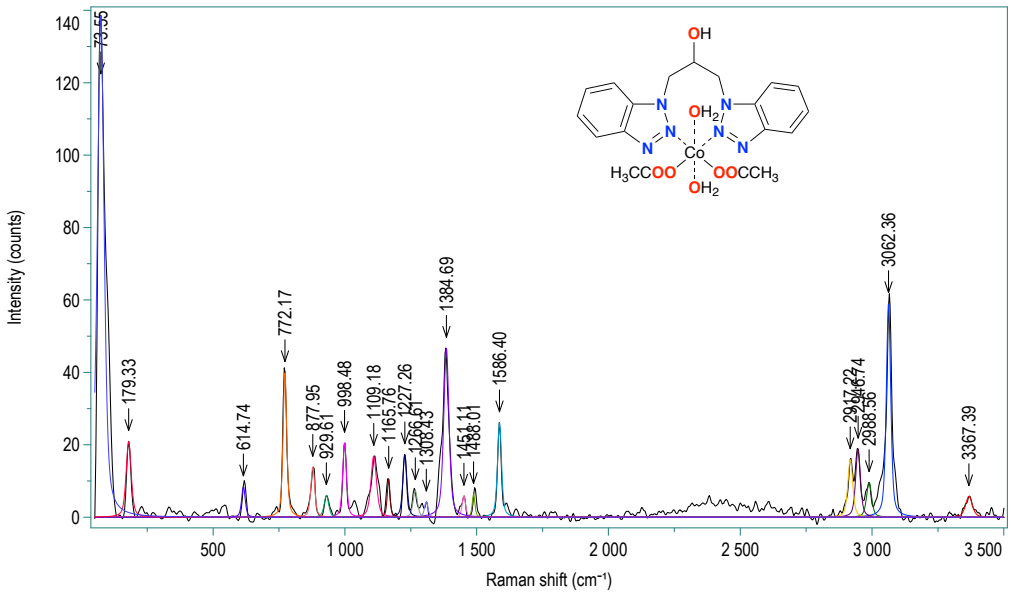


**Figure S14**. Raman spectrum of diacetate-diaqua-[1,3-bis(benzotriazole-1-yl)propan-2-ol-N,N']cobalt(II) (**4**)

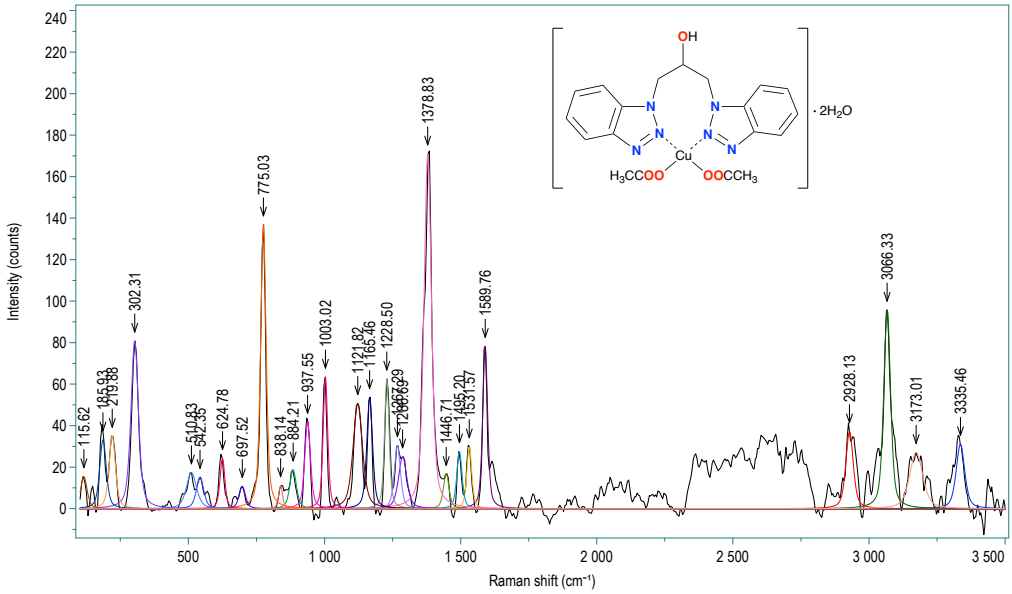


**Figure S15**. Raman spectrum of diacetate[1,3-bis(benzotriazole-1-yl)propan-2-ol-N,N']copper(II) dihydrated (**5**)

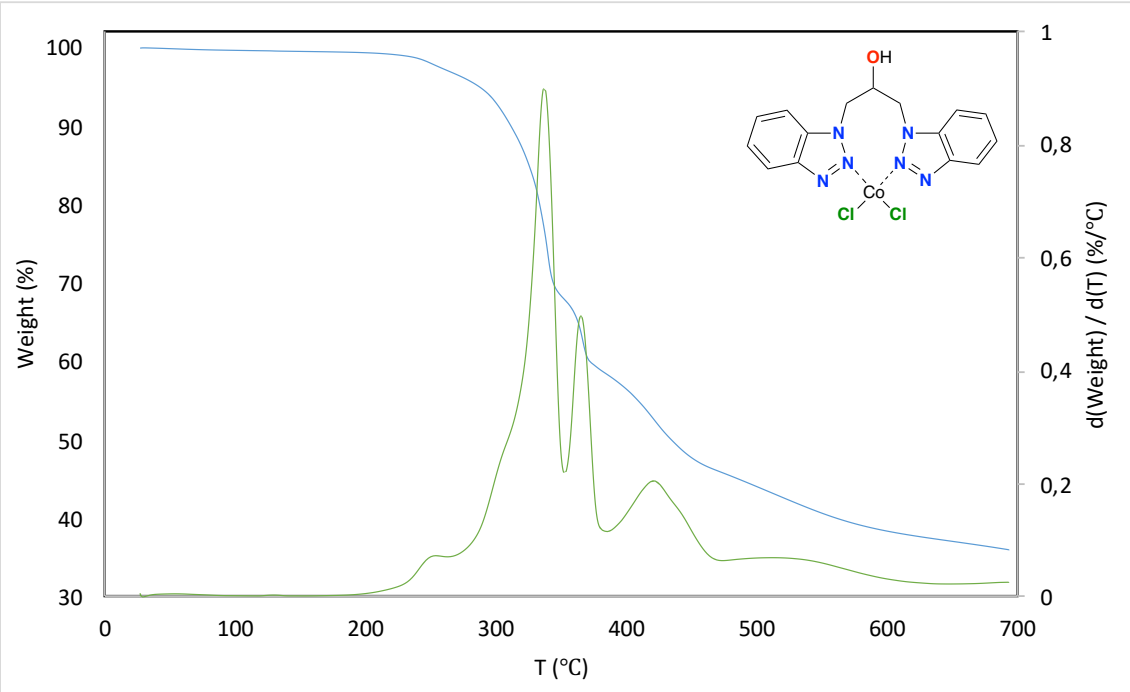


**Figure S16.** Thermogravimetric (TG) analysis and derivative thermogravimetric (DTG) of dichloro[1,3-bis(benzotriazole-1-yl)propan-2-ol-N,N']cobalt(II) (**2**) in nitrogen atmosphere

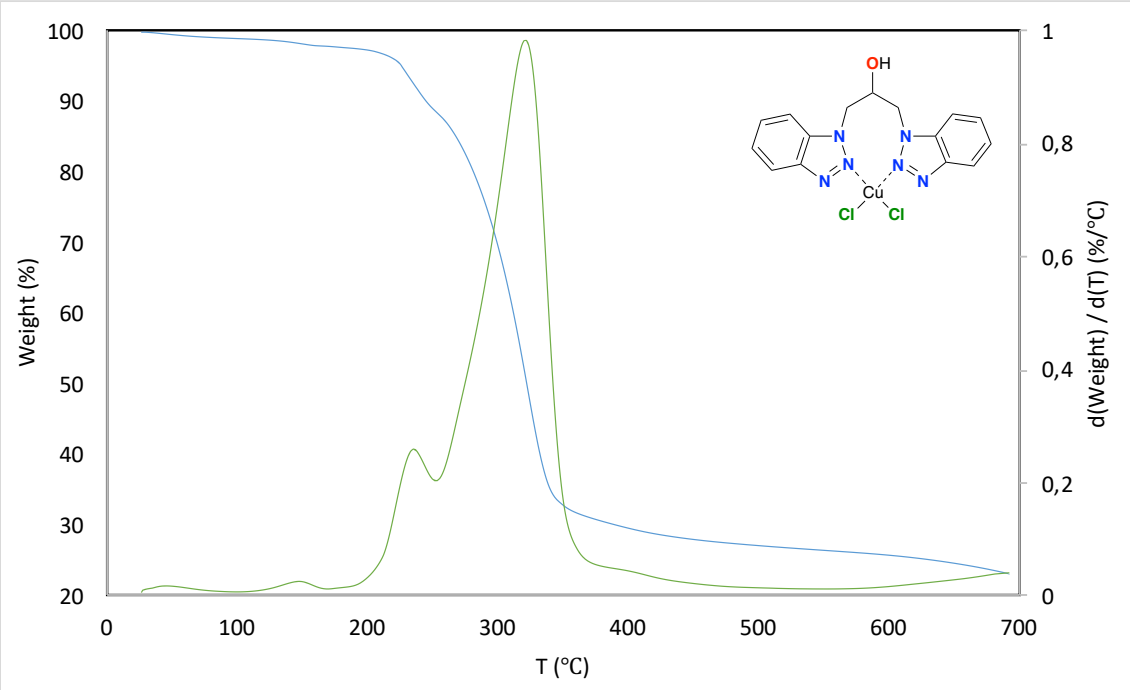


**Figure S17.** Thermogravimetric (TG) analysis and derivative thermogravimetric (DTG) of dichloro[1,3-bis(benzotriazole-1-yl)propan-2-ol-N,N']copper(II) (**3**) in nitrogen atmosphere

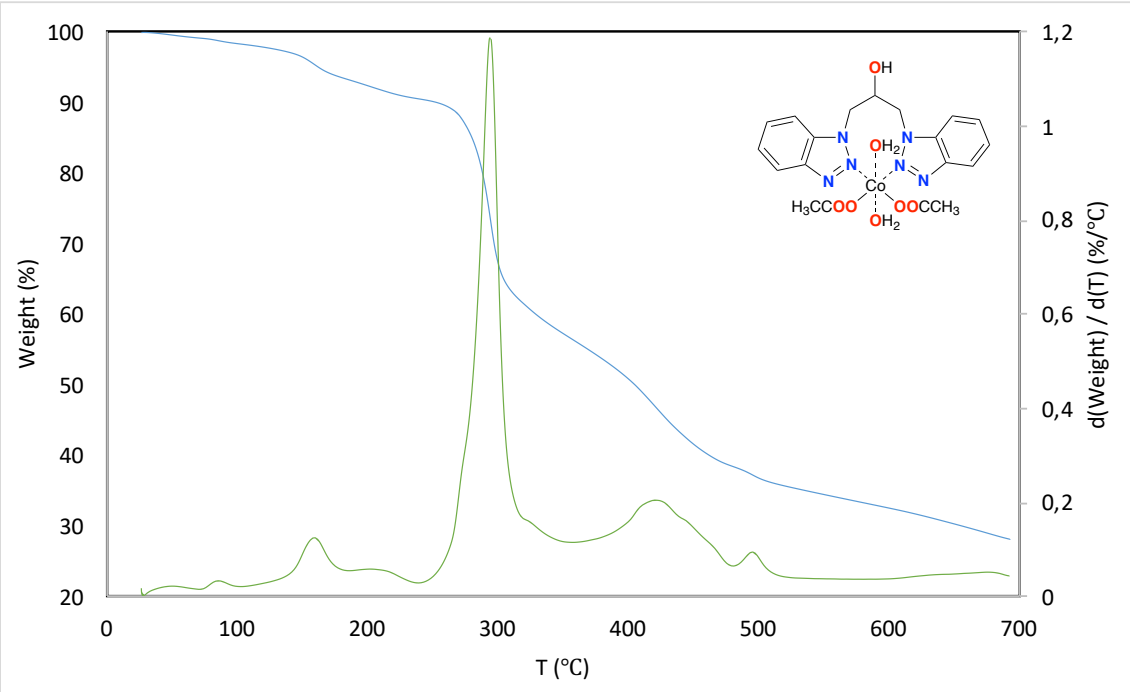


**Figure S18.** Thermogravimetric (TG) analysis and derivative thermogravimetric (DTG) of diacetate-diaqua-[1,3-bis(benzotriazole-1-yl)propan-2-ol-N,N']cobalt(II) (**4**) in nitrogen atmosphere

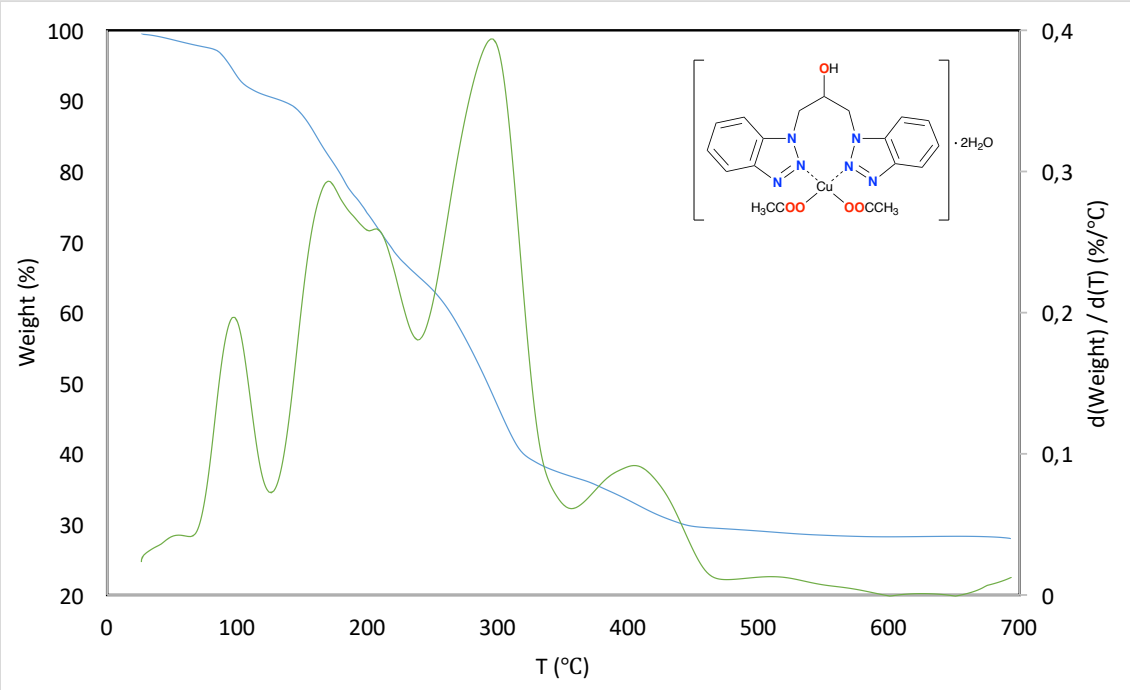


**Figure S19.** Thermogravimetric (TG) analysis and derivative thermogravimetric (DTG) of diacetate[1,3-bis(benzotriazole-1-yl)propan-2-ol-N,N']copper(II) dihydrated (**5**) in nitrogen atmosphere

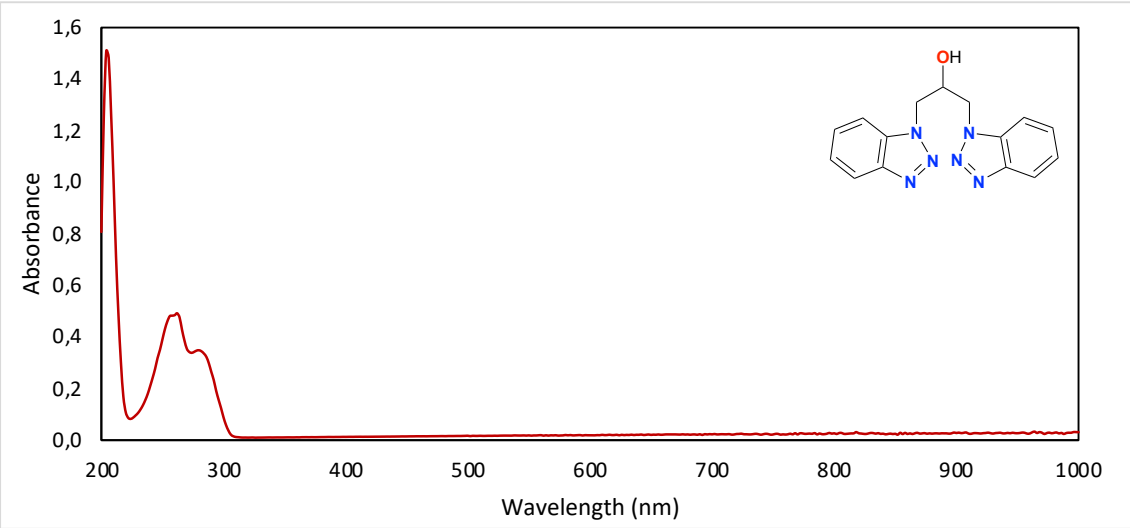


**Figure S20**. UV-Vis spectrum of 1,3-bis(benzotriazole-1-yl)propan-2-ol (**1**) in methanol. 2.10 x $10^{-5}$ M, 200-1000 nm region

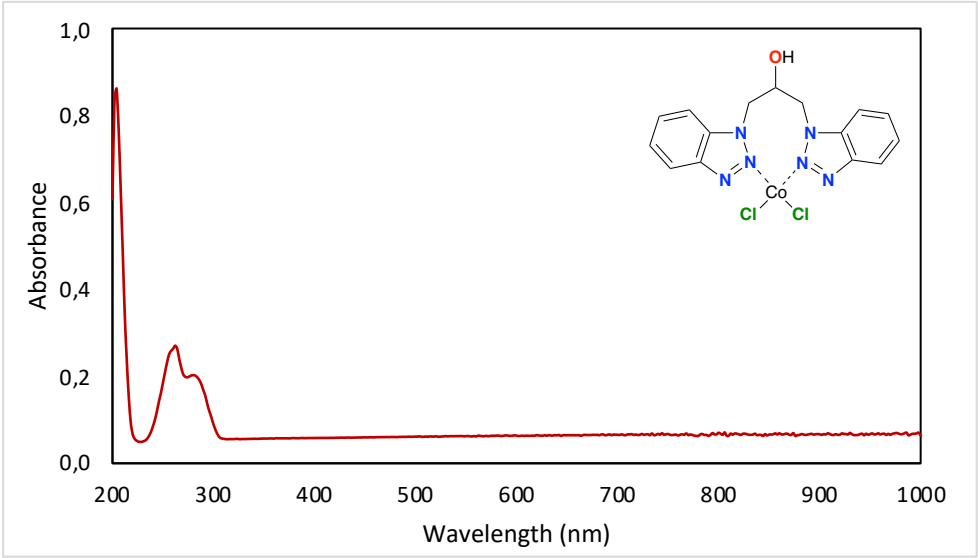


**Figure S21**. UV-Vis spectrum of dichloro[1,3-bis(benzotriazole-1-yl)propan-2-ol-N,N']cobalt(II) (**2**) in methanol. 2.18 x $10^{-5}$ M, 200-1000 nm region

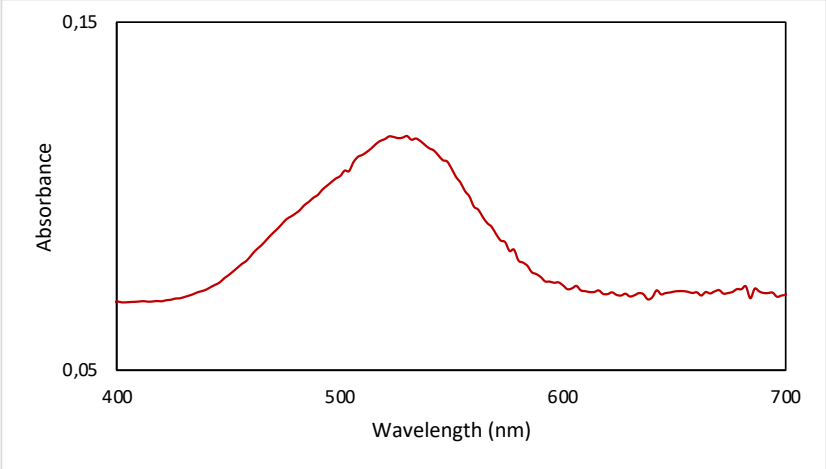


**Figure S22**. UV-Vis spectrum of dichloro[1,3-bis(benzotriazole-1-yl)propan-2-ol-N,N']cobalt(II) (**2**) in methanol. 4.72 x $10^{-3}$ M, 400-700 nm region

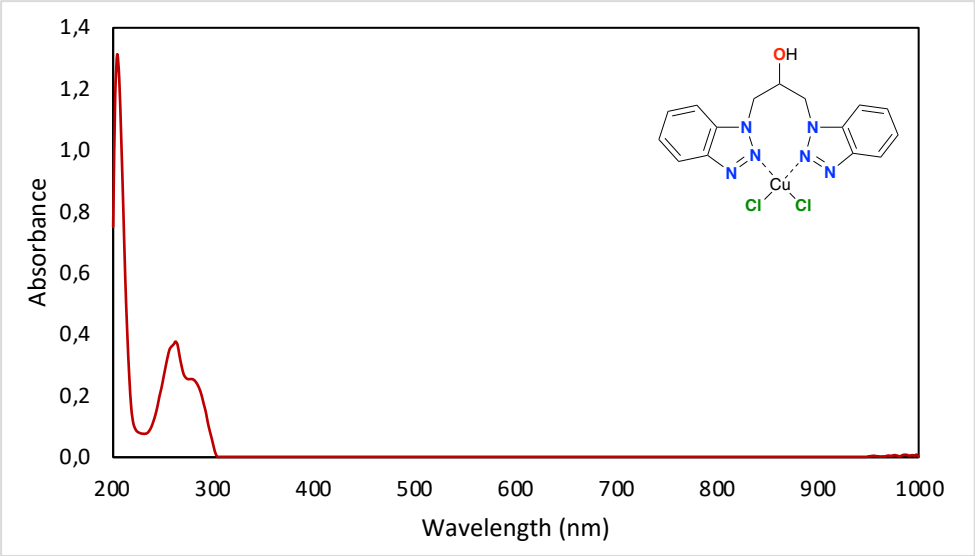


**Figure S23**. UV-Vis spectrum of dichloro[1,3-bis(benzotriazole-1-yl)propan-2-ol-N,N']copper(II) (**3**) in methanol. 2.16 x $10^{-5}$ M, 200-1000 nm region

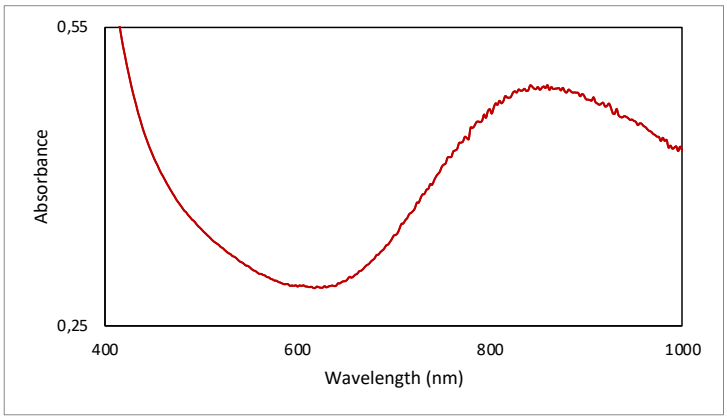


**Figure S24**. UV-Vis spectrum of dichloro[1,3-bis(benzotriazole-1-yl)propan-2-ol-N,N']copper(II) (**3**) in methanol. 4.66 x $10^{-3}$ M, 400-1000 nm region

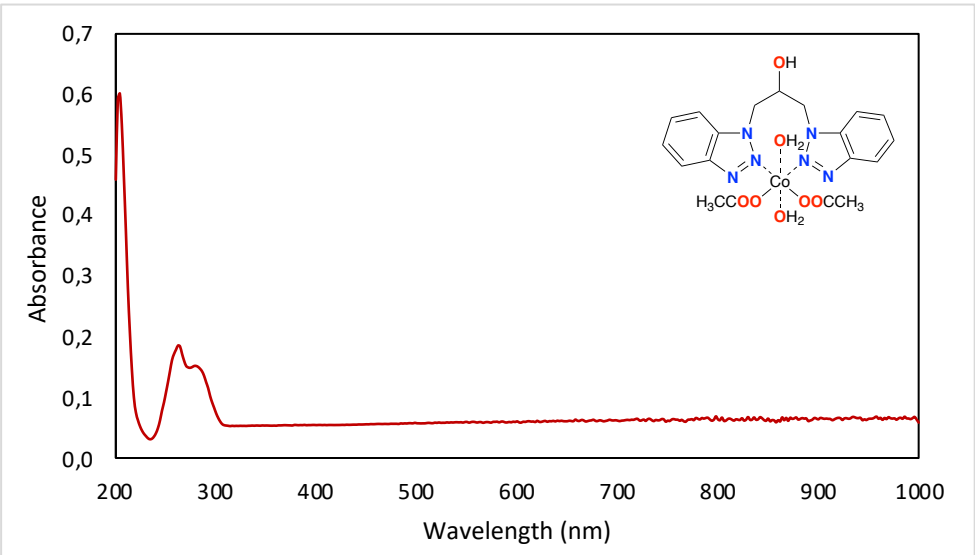


**Figure S25**. UV-Vis spectrum of diacetate-diaqua-[1,3-bis(benzotriazole-1-yl)propan-2-ol-N,N']cobalt(II) (**4**) in methanol. 1.82 x $10^{-5}$ M, 200-1000 nm region

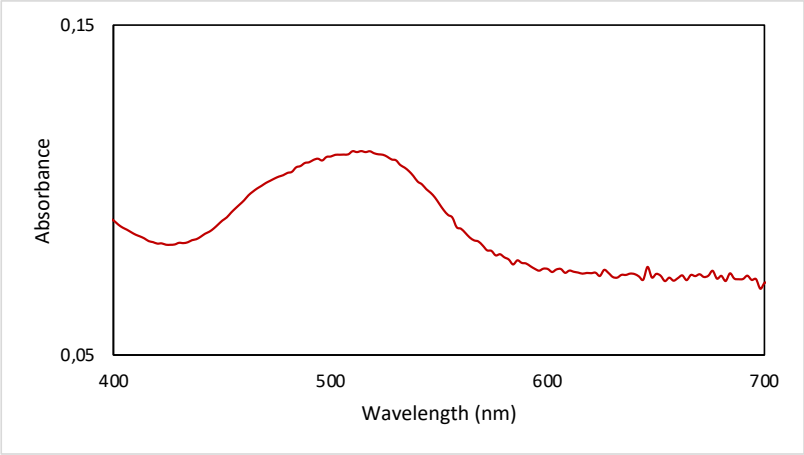


**Figure S26**. UV-Vis spectrum of diacetate-diaqua-[1,3-bis(benzotriazole-1-yl)propan-2-ol-N,N']cobalt(II) (**4**) in methanol. 3.94 x $10^{-3}$ M, 400-700 nm region

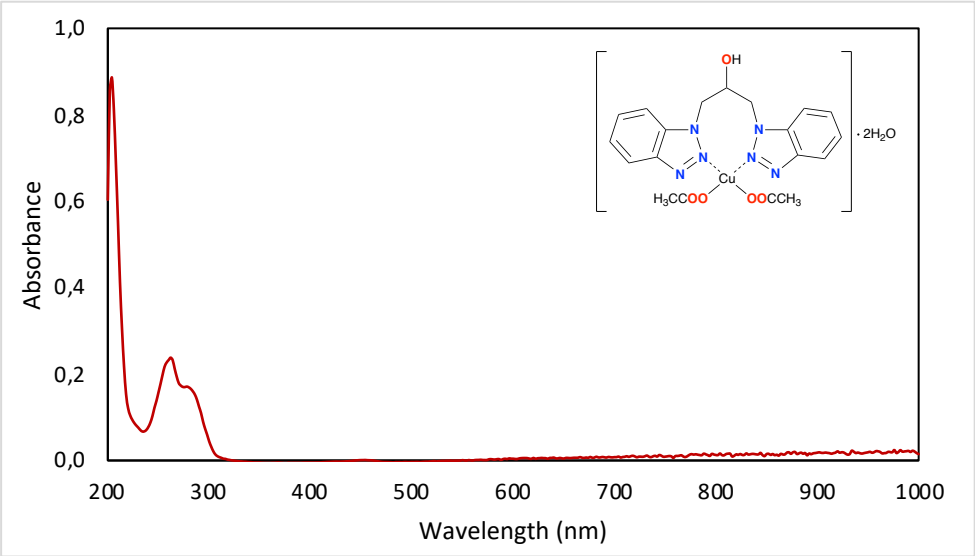


**Figure S27**. UV-Vis spectrum of diacetate[1,3-bis(benzotriazole-1-yl)propan-2-ol-N,N']copper(II) dihydrated (**5**) in methanol. 1.81 x $10^{-5}$ M, 200-1000 nm region

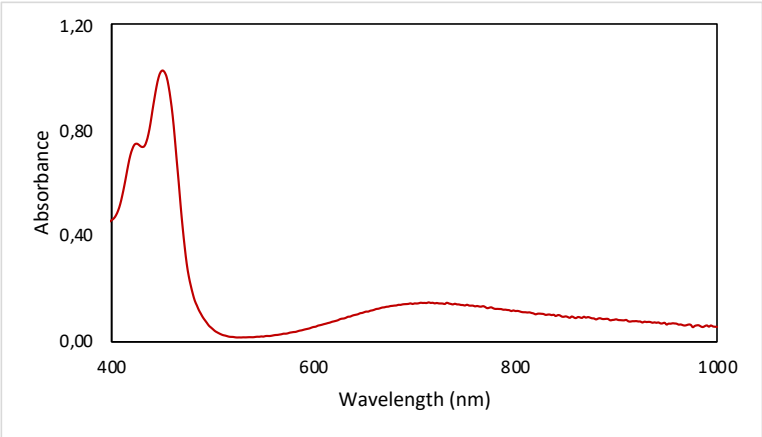


**Figure S28**. UV-Vis spectrum of diacetate[1,3-bis(benzotriazole-1-yl)propan-2-ol-N,N']copper(II) dihydrated (**5**) in methanol. 3.91 x $10^{-3}$ M, 400-1000 nm region

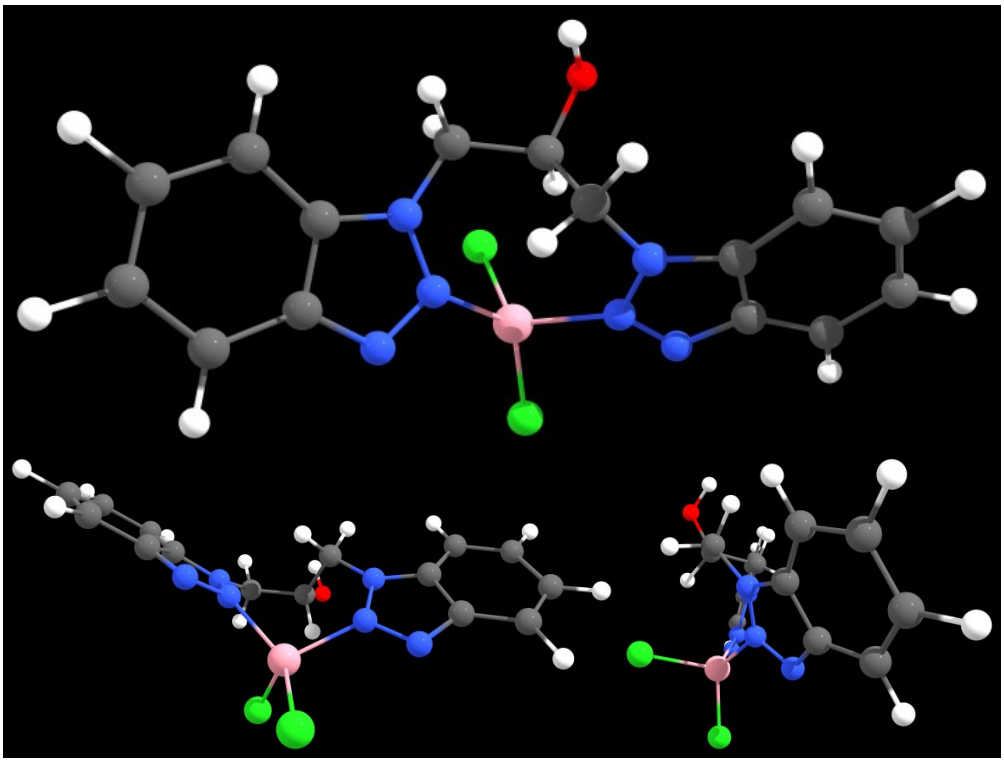

**Figure S29.** Optimized geometry of conformer Da of (**2**) – Different perspectives

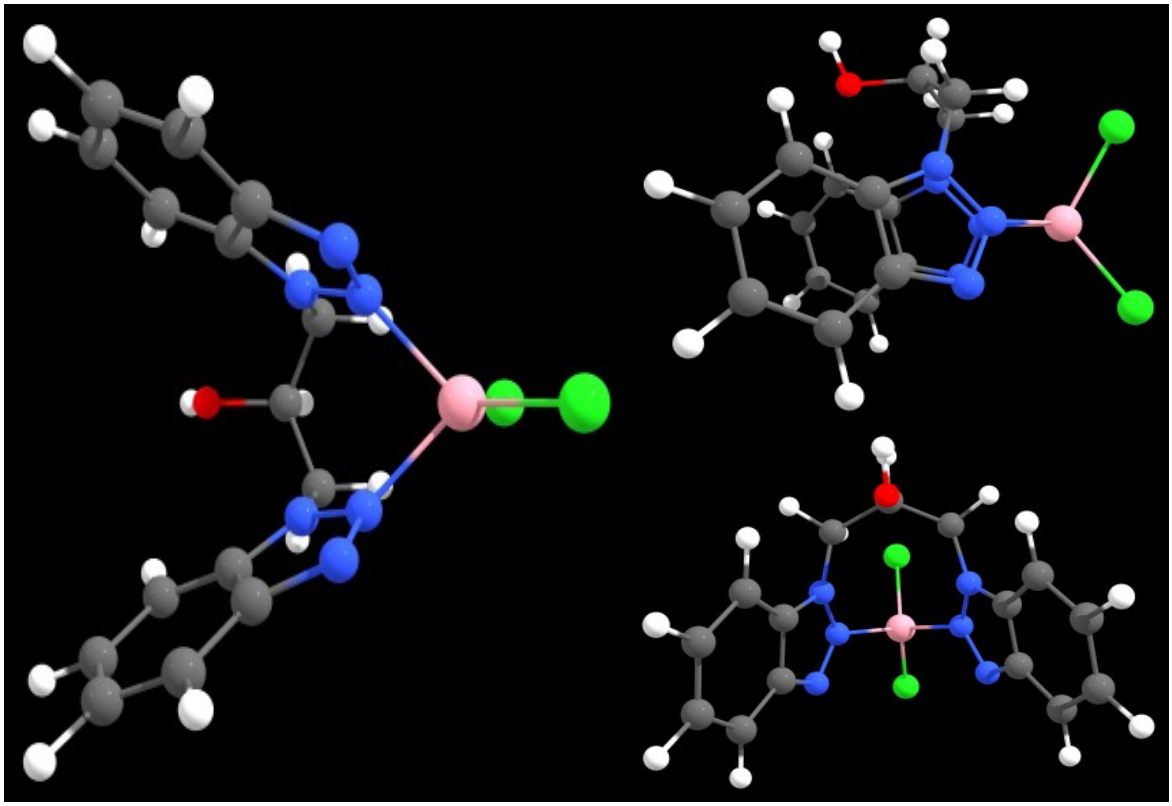

**Figure S30.** Optimized geometry of conformer Db of (**2**) – Different perspectives

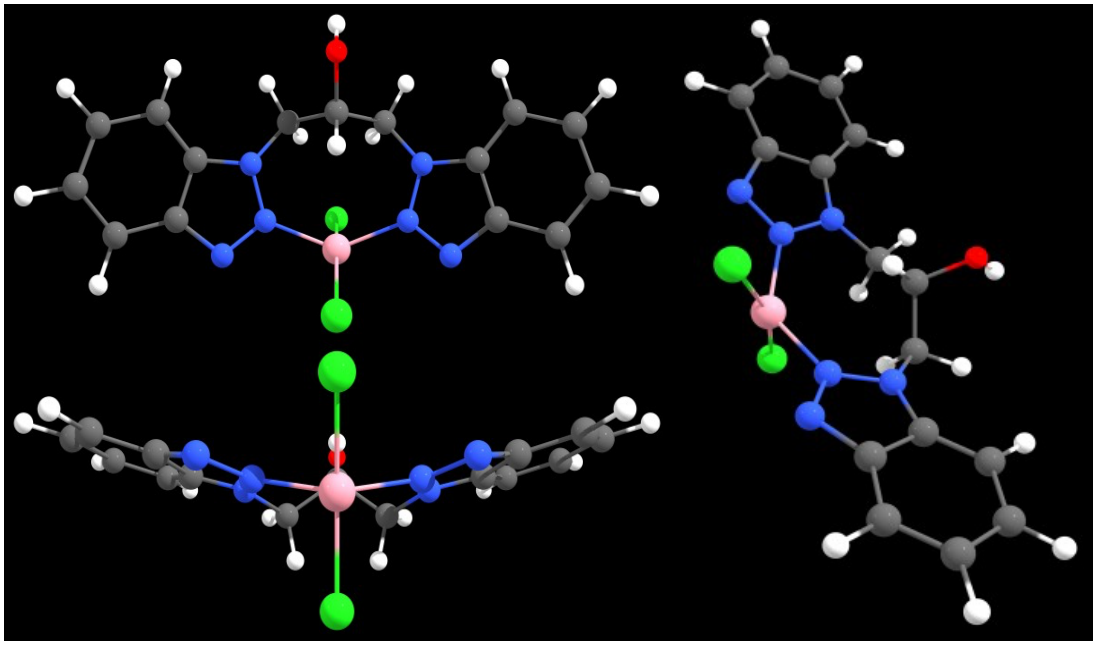

**Figure S31.** Optimized geometry of conformer Dc of (**2**) – Different perspectives

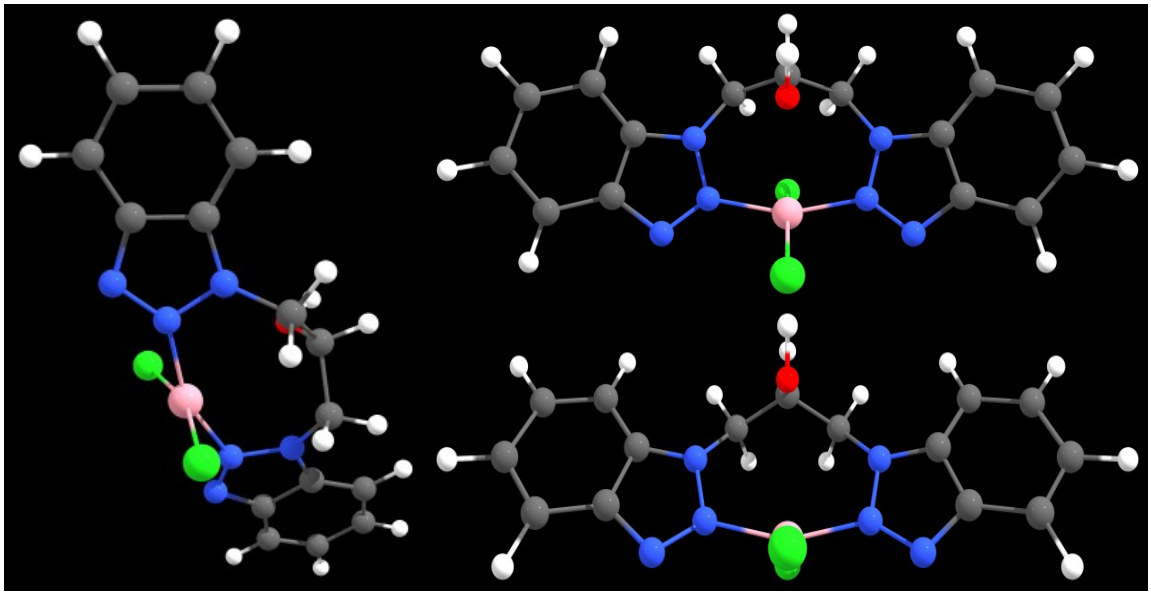

**Figure S32.** Optimized geometry of conformer Dd of (**2**) – Different perspectives

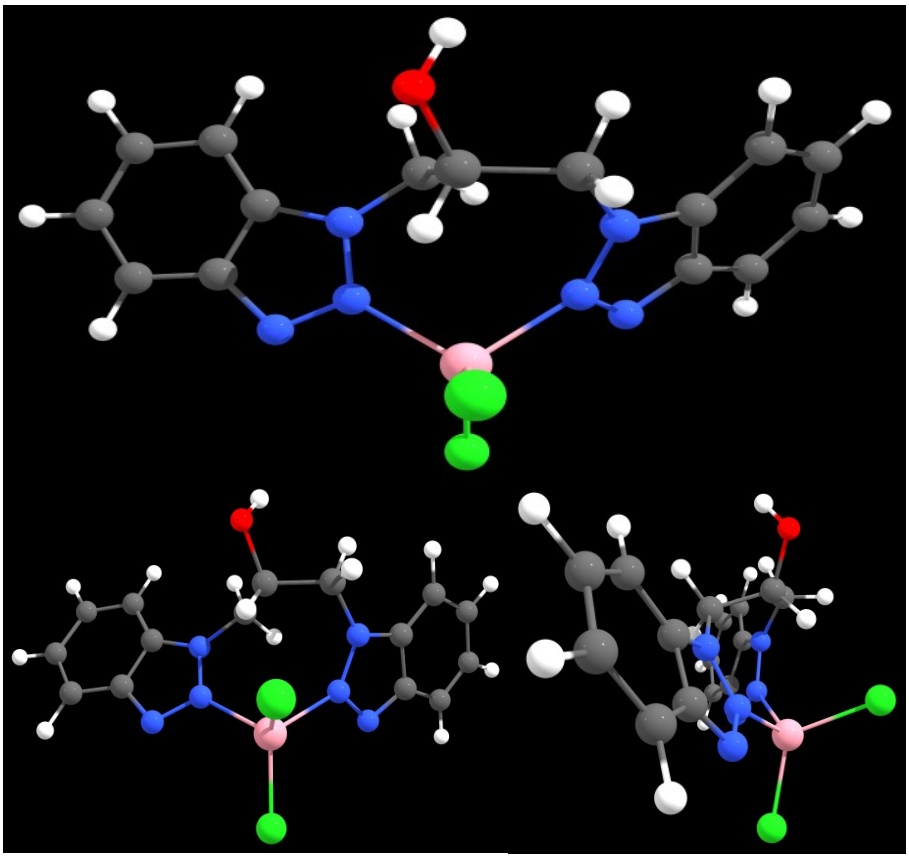

**Figure S33.** Optimized geometry of conformer Qa of (**2**) – Different perspectives

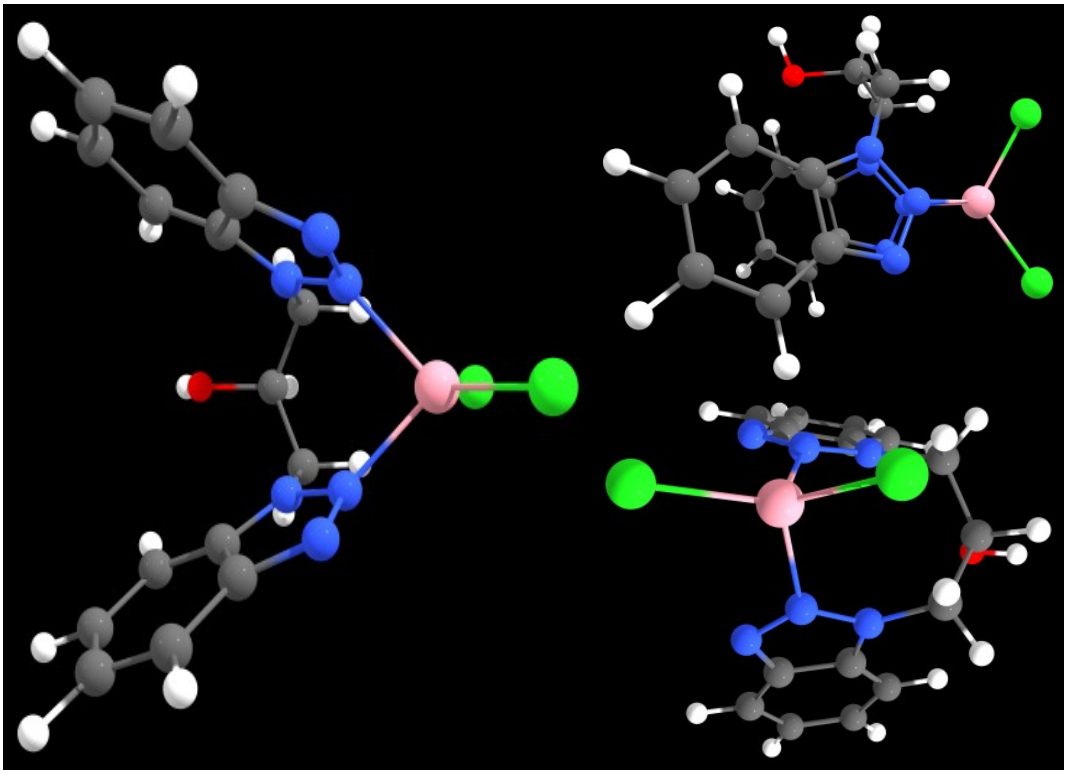

**Figure S34.** Optimized geometry of conformer Qb of (**2**) – Different perspectives

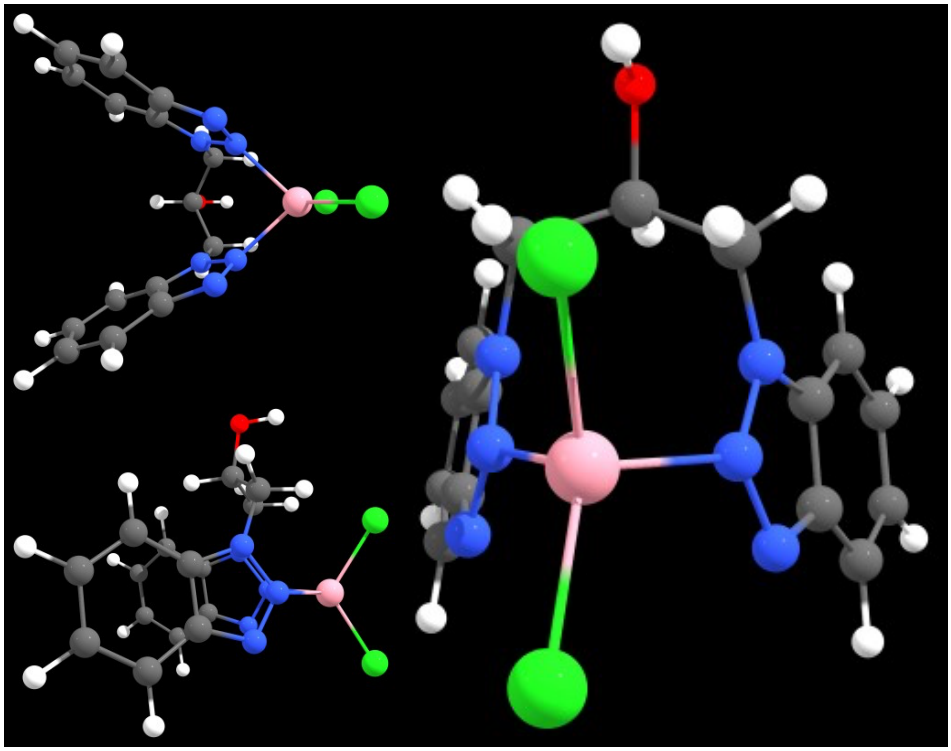

**Figure S35.** Optimized geometry of conformer Qc of (**2**) – Different perspectives

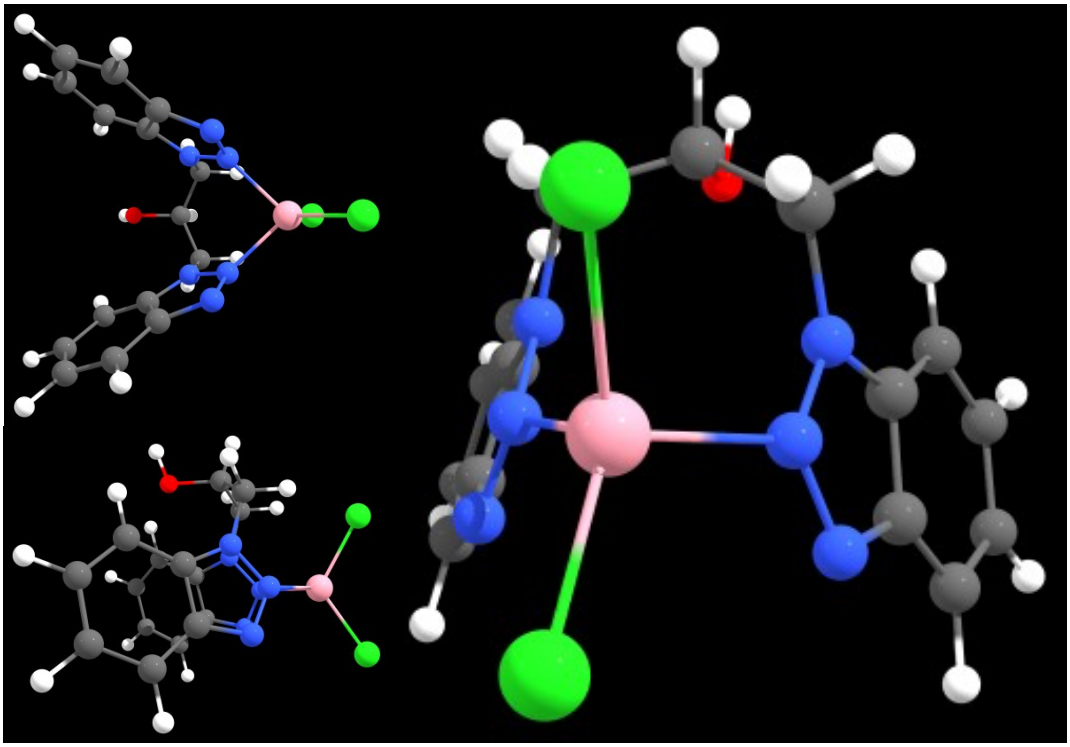

**Figure S36.** Optimized geometry of conformer Qd of (**2**) – Different perspectives

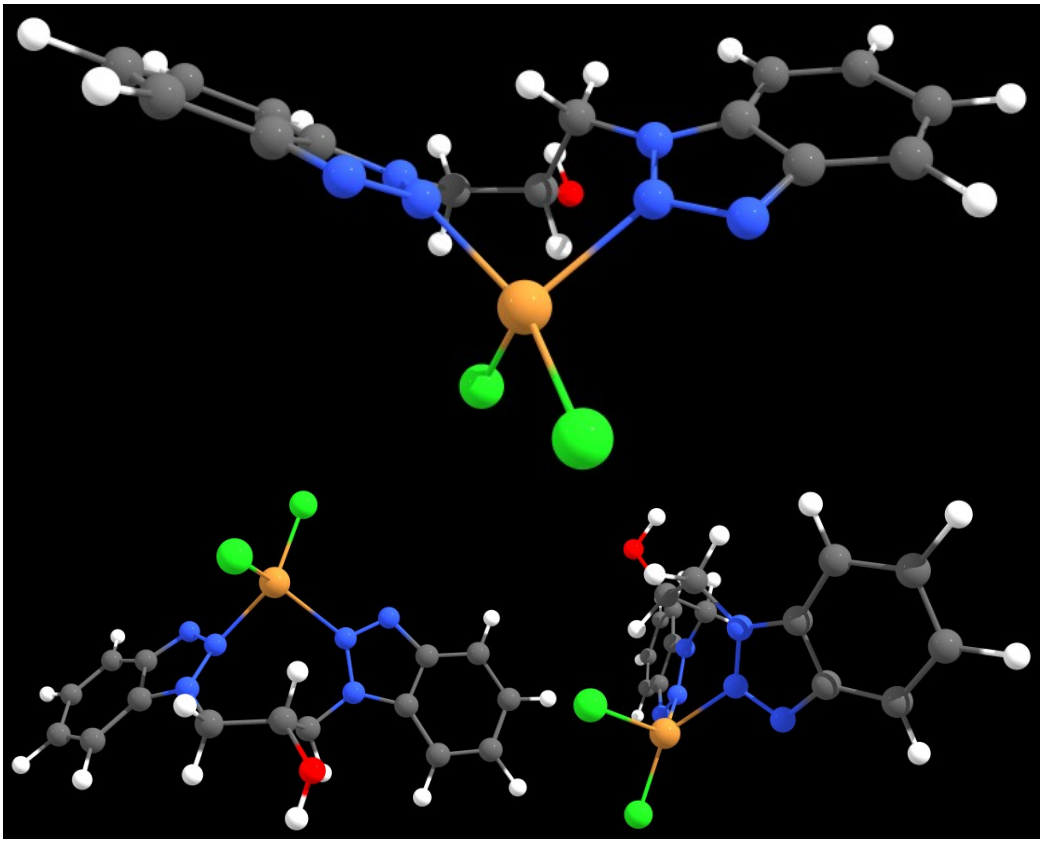

**Figure S37.** Optimized geometry of conformer Da of (**3**) – Different perspectives

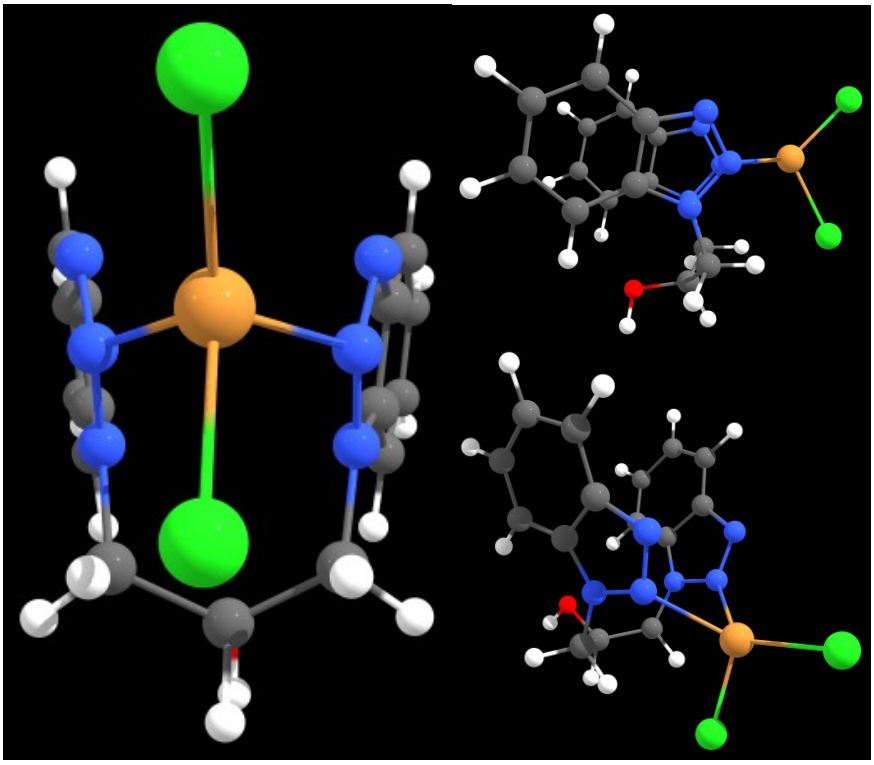

**Figure S38.** Optimized geometry of conformer Db of (**3**) – Different perspectives

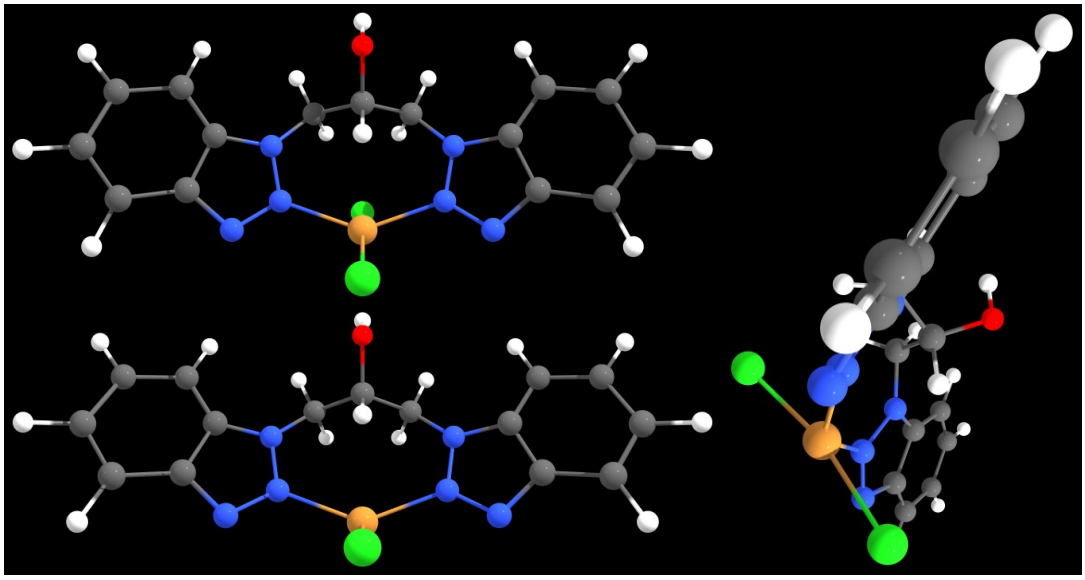

**Figure S39.** Optimized geometry of conformer Dc of (**3**) – Different perspectives

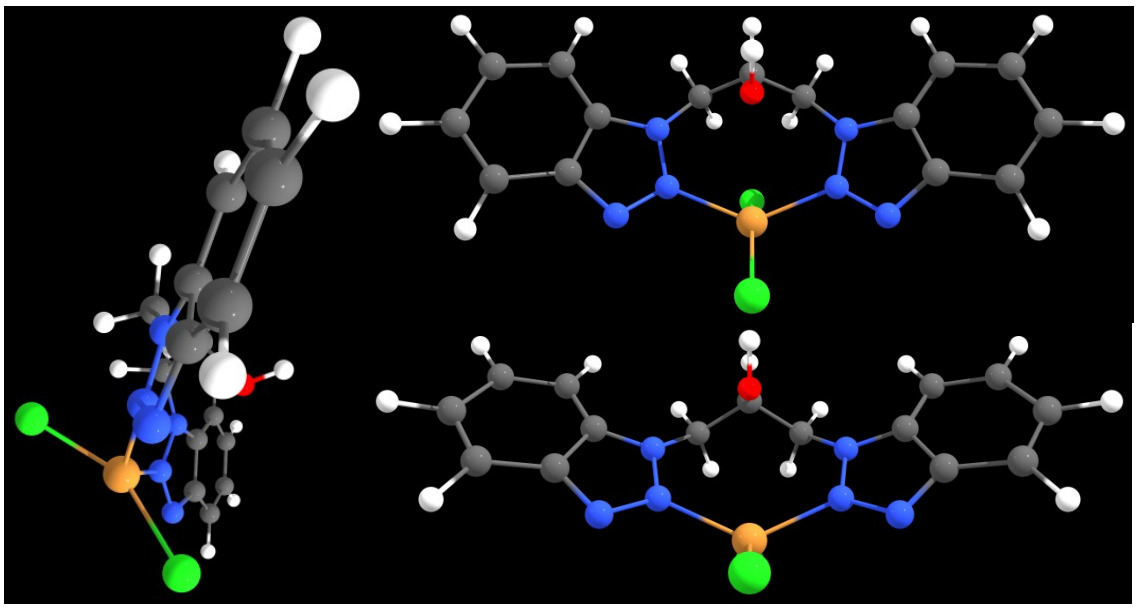

**Figure S40.** Optimized geometry of conformer Dd of (**3**) – Different perspectives

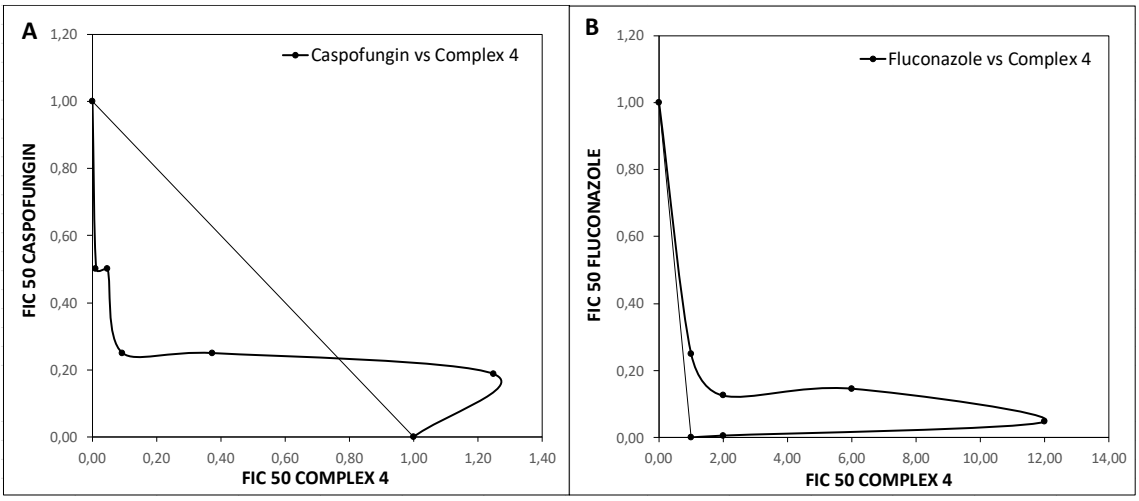


**Figure S41.** Drug interaction isobolograms. A: A (Caspofungin vs Complex 4 against *C. tropicalis* 66029) B (Fluconazole vs Complex 4 *C. albicans* 90028).

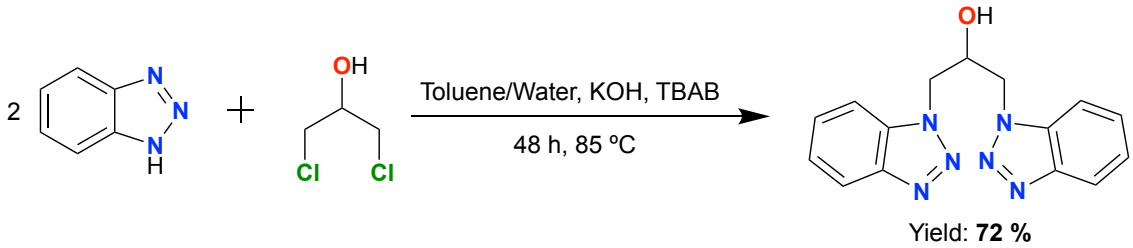


**Figure S42.** Synthesis of the ligand (**1**). TBAB = Tetrabutylammonium bromide

**Table S1.** Thermoanalytical results (TGA and DTG) for metal complexes.

| Compound (formula) | TG range / °C | $DTG_{max}$/ °C | | Mass loss | Total mass loss | Assignment | Metallic residue |
|---|---|---|---|---|---|---|---|
| | | | | **Estimated (calcd.) / %** | | | |
| | 152-352 | 254, 337 | 2 | 31.63 (31.63) | | loss of $C_6H_4N_3 + CH_4$ | |
| **2** | 352-385 | 365 | 1 | 9.52 (9.45) | 63.55 | loss of $C_3H_4$ | $CoCl_2CO$ |
| ($C_{15}H_{14}Cl_2CoN_6O$) | 385-473 | 421 | 1 | 12.53 (12.74) | (62.78) | loss of $CN_3$ | |
| | 473-694 | 512 | 1 | 9.86 (8.97) | | loss of $C_3H_2$ | |
| | 27-170 | 46, 148 | 2 | 1.99 (1.88) | | loss of $4H_2$ | |
| **3** | 170-253 | 236 | 1 | 9.25 (9.11) | 76.79 | loss of $C_3H_3$ | CuCl |
| ($C_{15}H_{14}Cl_2CuN_6O$) | 253-552 | 321 | 1 | 62.14 (62.41) | (76.91) | loss of $C_{11}N_6ClO$ | |
| | 552-694 | 694 | 1 | 3.40 (3.50) | | loss of $CH_3$ | |
| | 27-239 | 88, 159, 202 | 3 | 9.38 (9.47) | | loss of $2H_2O + C$ | |
| **4** | 239-358 | 294 | 1 | 34.10 (34.13) | 71.82 | loss of $C_6H_4N_3 + C_3H_3O$ | $CoC_2O_4$ |
| ($C_{19}H_{24}CoN_6O_7$) | 358-573 | 420, 495 | 2 | 22.81 (22.88) | (71.04) | loss of $C_6H_2N_3$ | |
| | 573-694 | 676 | 1 | 5.52 (4.55) | | loss of $CH_3 + 4H_2$ | |
| | 64-126 | 95 | 1 | 7.54 (7.43) | | loss of $2H_2O + H_2$ | |
| **5** | 126-239 | 170, 207 | 2 | 25.35 (25.42) | 70.06 | loss of $C_6H_4N_3 + C$ | $CuC_2O_4$ |
| ($C_{19}H_{24}CuN_6O_7$) | 239-357 | 296 | 1 | 28.37 (28.55) | (70.40) | loss of $C_6H_4N_3 + C_2H_4$ | |
| | 357-694 | 405 | 1 | 8.80 (8.99) | | loss of $C_2H_6O$ | |

**Table S2.** Antifungal activity of Co(II) and Cu(II) complexes containing 1,3-bis(benzotriazol-1-yl)-propan-2-ol on planktonic cells of *Candida sp*.

MIC: Minimum Inhibitory Concentration; CFM: Minimum fungicidal concentration. Measures expressed in μg $mL^{-1}$; ND: not determinated. The experiments were performed in triplicate at three independent times.

| **Compound** | ***C. albicans* ATCC 90028** | | ***C. albicans* CAP F-13** | | ***C. tropicalis* ATCC 66029** | | ***C. tropicalis* CAP F-01** | | ***C. glabrata* MYA2950** | | ***C. glabrata* CAPF-07** | | ***C. parapsilosis* ATCC22019** | | ***C. parapsilosis* 24754** | |
|---|---|---|---|---|---|---|---|---|---|---|---|---|---|---|---|---|
| | **MIC** | **CFM** | **MIC** | **CFM** | **MIC** | **CFM** | **MIC** | **CFM** | **MIC** | **CFM** | **MIC** | **CFM** | **MIC** | **CFM** | **MIC** | **CFM** |
| 1 | >1000 | >1000 | >1000 | >1000 | >1000 | >1000 | >1000 | >1000 | >400 | >400 | >1000 | >1000 | >1000 | >1000 | >1000 | >1000 |
| 2 | 125 | 250 | 125 | 500 | 125 | 1000 | 62.5 | 500 | 25 | 100 | 62.5 | 62.5 | 62.5 | 125 | 62.5 | 500 |
| 4 | 62.5 | 125 | 62.5 | >1000 | 62.5 | 250 | 62.5 | 500 | 15.62 | 62.5 | 62.5 | 500 | 62.5 | 250 | 62.5 | 500 |
| 3 | >1000 | >1000 | >1000 | >1000 | 500 | >1000 | 1000 | >1000 | >400 | >400 | >1000 | >1000 | 125 | >1000 | >1000 | >1000 |
| 5 | >1000 | >1000 | >1000 | >1000 | 500 | >1000 | 500 | >1000 | >250 | >250 | 1000 | >1000 | >1000 | >1000 | 500 | >1000 |
| S2 | 31.25 | 62.5 | 31.25 | 250 | 31.25 | 125 | 7.81 | 62.5 | 15.62 | 31.25 | 15.6 | 62.5 | 31.25 | 62.5 | 15.6 | 125 |
| S4 | 62.5 | 125 | 62.5 | >1000 | 31.25 | 125 | 31.25 | 125 | 15.65 | 31.25 | 15.6 | 62.5 | 31.25 | 125 | 15.6 | 62.5 |
| S3 | 1000 | >1000 | 125 | >1000 | 250 | 1000 | 125 | 1000 | >250 | >250 | 125 | >1000 | >1000 | >1000 | 250 | >1000 |
| S5 | 1000 | >1000 | 125 | >1000 | 125 | >1000 | 125 | >1000 | >250 | >250 | 250 | >1000 | >1000 | >1000 | 125 | 1000 |
| Fluconazole[1] | 0.25 | >64 | 32 | >64 | 2.0 | >32 | 32 | >64 | 0.5 | 0.5 | 64 | >64 | 1.0 | >64 | 32 | >64 |
| Itraconazole[2] | 0.03 | 16 | 0.5 | >16 | >16 | >16 | 0.5 | >16 | 0.5 | 0.5 | 4 | >16 | 0.0625 | 4 | >16 | >16 |
| Caspofungin | 0.062 | 0.125 | 0.062 | 0.062 | 0.125 | 0.125 | 1.0 | 4 | ND | ND | ND | ND | ND | ND | ND | ND |

**Table S3.** Matrix of combinations between cobalt(II) complexes and reference drugs (FCZ and Caspofungin).

| Combination | Drug A (Complexes) | Drug B (Reference drugs) |
|---|---|---|
| 1 | 8X MIC | 0 |
| 2 | 4X MIC | 1/4 MIC |
| 3 | 2X MIC | 1/2 MIC |
| 4 | MIC | MIC |
| 5 | 1/2 MIC | 2X MIC |
| 6 | 1/4 MIC | 4X MIC |
| 7 | 0 | 8X MIC |